Proc. Natl. Acad. Sci. USA
Vol. 95, pp. 2950–2955, March 1998
Cell Biology

Centrosome hypertrophy in human breast tumors: Implications for genomic stability and cell polarity

WILMA L. LINGLE, WARD H. LUTZ, JAMES N. INGLE, NITA J. MAIHLE, AND JEFFREY L. SALISBURY*

Tumor Biology Program, Mayo Clinic Foundation, Rochester, MN 55905

Communicated by Bruce Alberts, National Academy of Sciences, Washington, DC, January 7, 1998 (received for review September 5, 1997)

ABSTRACT **The centrosome plays an important role in maintenance of cell polarity and in progression through the cell cycle by determining the number, polarity, and organization of interphase and mitotic microtubules. By examining a set of 35 high grade human breast tumors, we show that centrosomes of adenocarcinoma cells generally display abnormal structure, aberrant protein phosphorylation, and increased microtubule nucleating capacity in comparison to centrosomes of normal breast epithelial and stromal tissues. These structural and functional centrosome defects have important implications for understanding the mechanisms by which genomic instability and loss of cell polarity develop in solid tumors.**

The centrosome functions as the major microtubule organizing center (MTOC) of interphase and mitotic cells (1). Mammalian centrosomes consist of a pair of centrioles surrounded by a pericentriolar matrix (2–5). For many cell types, including epithelial cells, the position of the centrosome relative to the nucleus defines a structural "cell axis" [first recognized by Van Beneden in 1883 (see ref. 6)] that indicates the overall functional polarity of the cell (7). This functional polarity is maintained, in part, by the organization of the microtubule array that originates at the centrosome and by directional vesicular trafficking that proceeds along these microtubules (8). Once in each cell cycle, typically around the time of the G_1/S transition, the centrosome duplicates itself (1). At G_2/M, duplicated centrosomes separate to give rise to two mitotic spindle poles that organize the mitotic apparatus. A growing number of centrosomal proteins has been identified for which both function and sequence information are known. These include: centrin, which functions in centrosome duplication and separation (9–11); γ-tubulin, a unique member of the tubulin family that plays a role in microtubule nucleation (12–15); and pericentrin, a protein involved in organizing centrosome structure (16, 17). Centrin is located within the centrioles themselves and, along with γ-tubulin and pericentrin, is also a component of the pericentriolar material that surrounds the centrioles (13, 18, 19).

Early in this century, Theodor Boveri proposed that the characteristic loss of cell polarity and chromosomal segregation abnormalities (aneuploidy) seen in malignant tumors could result from defects in centrosome function (20). This proposal is supported by several recent studies implicating mutations in the tumor suppressor gene product p53 in the accumulation of genetic defects (21) and in disregulation of centrosome duplication during the cell cycle (22–24). Boveri's original proposal was based on studies of abnormal development in sea urchin embryos after double fertilization. This hypothesis, however, never has been examined by using human tumor samples. We, therefore, performed a careful examination of centrosomes in 35 human breast carcinomas and five normal breast specimens to determine if structural and functional centrosome abnormalities are characteristic of cancer cells *in situ.* These studies demonstrate that breast adenocarcinoma centrosomes display characteristic structural alterations, including: (*i*) an increase in centrosome number and volume, (*ii*) accumulation of excess pericentriolar material, (*iii*) supernumerary centrioles, and (*iv*) inappropriate phosphorylation of centrosomal proteins. In addition, by using a microtubule nucleation assay, we demonstrate that breast tumor cells show functional centrosome abnormalities characterized by increased numbers of MTOCs nucleating unusually large arrays of microtubules. These observations have important implications for understanding the mechanisms underlying genomic instability and loss of cell polarity characteristic of high grade tumors.

MATERIALS AND METHODS

Human Tissue Samples and Cell Culture. Human breast tissues were obtained immediately after surgery under an institutional review board-approved protocol, frozen in liquid nitrogen, and stored at −70°C. For some studies, unfrozen tissue was processed immediately for electron microscopy (see below). Five breast adenocarcinoma specimens selected at random from 135 frozen tumors were studied in detail. Thirty additional tumor specimens were surveyed independently for centrosome characteristics as described below. All tumors were designated as histological grade 4 (Mayo grading system) at the time of surgery by staff pathologists and were frankly metastatic based on lymph node involvement. Specimens were obtained from patients who had no chemotherapeutic or radiation treatments before surgery. Normal tissues from five reduction mammoplasties that showed no indication of malignant pathology also were studied. The immortal human breast cell line MCF10A was cultured in DMEM supplemented with 10% fetal calf serum, 10 μg/ml insulin, and 30 ng/ml epidermal growth factor (25).

Centrosome Staining and Analysis. Cryosections (≈12 μm thick) of breast tissue mounted on coated slides were fixed in −20°C methanol, blocked in PBS (containing 5% normal goat serum, 1% glycerol, 0.1% BSA, and 0.1% fish skin gelatin), and stained by using anti-centrin mAb 20H5 (1:800 dilution of mouse ascites) followed by a fluorescein isothiocyanate secondary antibody (1:800 goat anti-mouse, Cappel) and propidium iodide (2.5 ng/ml) for DNA. Some specimens also were stained with a polyclonal antibody against centrin (14/26–1, 1:500 dilution of serum) or γ-tubulin (1:500 dilution of serum, a gift of H. Joshi, Atlanta, GA). Samples were observed by using a Nikon FXA epifluorescence microscope or a Zeiss LSM 310 scanning laser confocal microscope, and images were recorded either by using Kodak Elite II color slide film or

The publication costs of this article were defrayed in part by page charge payment. This article must therefore be hereby marked "*advertisement*" in accordance with 18 U.S.C. §1734 solely to indicate this fact.

Abbreviations: MTOC, microtubule organizing center; HPC, human phosphocentrin peptide.

*To whom reprint requests should be addressed. e-mail: salisbury@mayo.edu.

electronically. For quantitative digital analysis of centrin staining, 16 consecutive 0.5- μm optical sections were collected by confocal microscopy to yield a total image stack with a volume of $8 \times 51 \times 51$ μm^3. Raw digital fluorescence data were imported into Analyze, an image processing program (Mayo Foundation, Rochester, MN), and signal intensity threshold was adjusted so that centrin-labeled spots were discrete objects in the green channel and nuclei were discrete objects in the red channel. Threshold-adjusted volume data were converted into binary files and imported into AVW (Mayo Foundation) to generate counts and volumes of centrin-staining spots.

Electron Microscopy. Normal breast tissue from a reduction mammoplasty and a grade 4 tumor specimen were prepared for electron microscopy. Freshly excised tissue was cut into cubes $\approx$1 mm^3, fixed overnight (4% formaldehyde and 1% glutaraldehyde in sodium phosphate buffer, pH 7.2), processed for transmission electron microscopy, sectioned and stained with uranyl acetate and lead citrate, and observed on a Philips CM10 Biotwin electron microscope (Philips Electronic Instruments, Mahwah, NJ). For counts of centriole profiles, electron micrographs of sections through normal and tumor cells were taken at random. By using negatives, each epithelial cell was scored for the number of centriole profiles present in that plane of section. Counts were made for 115 normal and 111 tumor cells. Observations also were made on a series of consecutive serial sections to determine total centriole counts for selected individual cells.

Microtubule Nucleation Assay. Cryosections of breast tissues mounted on coated coverslips were permeabilized for 10 min with chilled microtubule stabilizing buffer (1% Triton X-100/10 mM Pipes/2 mM EGTA/1 mM $MgSO_4$, pH 7.2) and washed several times with buffer without detergent. Cold reaction mixture, consisting of 15% (vol/vol) cytostatic factor-arrested *Xenopus* egg extract (26) diluted in microtubule stabilizing buffer with 1 mM GTP, was applied to the sections and incubated on ice for 10 min. The coverslips then were incubated at 28°C for 7 min to initiate microtubule nucleation and growth. The reaction was stopped by dilution, and microtubules were stabilized with taxol before fixation in -20°C methanol for 10 min followed by a second fixation in 2% paraformaldehyde for 5 min. Alternatively, touch preparations were made by pressing a coverslip against a 30-μm thick cryosection of tissue. Individual epithelial cells transferred out of the tissue section and stuck to the coverslip, leaving behind connective tissue elements that otherwise interfere with microtubule visualization. Transferred cells were processed for microtubule nucleation as described above. Sections and touch preparations were immunolabeled for tubulin, and nuclei were stained with propidium iodide and 4′,6-diamidino-2-phenylindole. Interphase cells from touch preparations were used to generate the microtubule counts presented in Table 1*C*.

Preparation and Analysis of Phosphocentrin-Specific Antibodies. A peptide (cEEFLRIMKKTSLY) corresponding to the carboxyl-terminal 13 amino acid residues of human centrin (9) was synthesized according to Morbeck and coworkers (27). The free serine hydroxyl group corresponding to serine 170 in the intact protein was phosphorylated by using "global" phosphite–triester phosphorylation (28) to yield the human phosphocentrin peptide (HPC) cEEFLRIMKKTS^{P}LY. Female New Zealand white rabbits were immunized with HPC conjugated to keyhole limpet hemocyanin. Antibodies against HPC (αHPC) were affinity purified on HPC-conjugated chromatography Sulfolink resin (Pierce). Bacterially expressed recombinant human centrin (29) was phosphorylated *in vitro* by using protein kinase A and [γ-^{32}P]ATP under conditions that yielded approximately half of the centrin as phosphorylated product. Tryptic peptide mapping and phosphoamino acid analysis demonstrated that only the serine corresponding to the residue at position 170 in the intact protein was phosphorylated under these conditions (W.H.L. and J.L.S., unpublished observations). Phosphorylated and nonphosphorylated centrin were resolved by SDS/PAGE and transferred to Immobilon-P (Millipore) membrane for Western analysis and autoradiography. Confirmation of centrin phosphorylation in human breast tumors was made by analyzing whole cell extracts of tumor tissue by using αHPC Western blot.

Table 1. Quantitative analysis of normal and tumor centrosomes

A	Analysis of centrin staining volume			
Tissue	Mean μm^3 (SD)	Vol. per cell μm^3 (SD)	*n* spots per cell (SD)	*n*
Normal	0.013 (0.004)	0.011 (0.002)	1.5 (0.3)	327
Tumor	0.114 (0.022)	0.492 (0.209)	4.3 (1.2)	1283

B	Analysis of centriole profiles per thin section		
Tissue	Mean	Range	*n*
Normal	0.061	0–2	115
Tumor	0.63	0–5	111

C	Microtubules nucleated per cell, *n*			
Tissue	Median	Mean number	Range	*n*
Normal	1	4.8	0–52	150
Tumor	39.7	47.1	0–270	150

RESULTS

A terminal duct from normal inactive breast tissue, consisting of distinctly polarized cuboidal epithelial cells and surrounding myoepithelial cells, is illustrated in Fig. 1*A*. Centrosome position was determined for normal ductal epithelial cells by using indirect immunofluorescence staining of the centrosomal protein centrin (Fig. 1*B*). In normal breast tissues, centrin labeling is restricted to the pair of centrioles located above the nucleus, very near the luminal membrane, in each cuboidal epithelial cell (see quantitative analysis below). Centrioles of all normal breast tissue cell types, including epithelial cells, myoepithelial cells, fibroblasts, and vascular endothelial cells, showed comparable levels of centrin immunostaining. Likewise, regions of normal tissue adjacent to breast tumors showed normal centrosome staining patterns.

In contrast, individual tumor cells of invasive adenocarcinomas displayed a characteristic loss of structural differentiation, a high nuclear-to-cytoplasmic ratio, and nuclear pleomorphism (Fig. 1*D*). Tumor cell centrosomes were present in greater numbers, and they were located chaotically within the cytoplasm compared with normal cells (Fig. 1*E*). Moreover, centrin localization in tumor cells was not restricted to the centrioles as it is in normal epithelial tissues (compare normal Fig. 1 *B–C* and tumor Fig. 1 *E–F*); in tumor cells, centrin staining also was seen as an extensive labeling of pericentriolar material.

Quantitative analysis demonstrated significant differences in centrosome number and volume between normal and tumor cells (Table 1). Results of a detailed analysis of three normal breast tissue specimens and five high grade breast adenocarcinomas are presented here. The mean volume for centrin-staining spots in normal epithelial cells is 0.013 μm^3, which is the volume of a centriole calculated from its physical dimensions [$\pi \times (0.1\ \mu m)^2 \times 0.4\ \mu m = 0.013\ \mu m^3$]. In contrast, the mean volume of centrin-stained spots analyzed in five separate tumor samples ranged from 0.092 to 0.138 μm^3 (overall mean for all five tumor samples = 0.114 μm^3), $\approx$7–10$\times$ the value observed for centrosomes in normal cells. On a per nucleus basis, the differences were even larger, with over 40 times the centrosome volume in tumor compared with normal cells. These volume differences in centrin staining for normal vs.

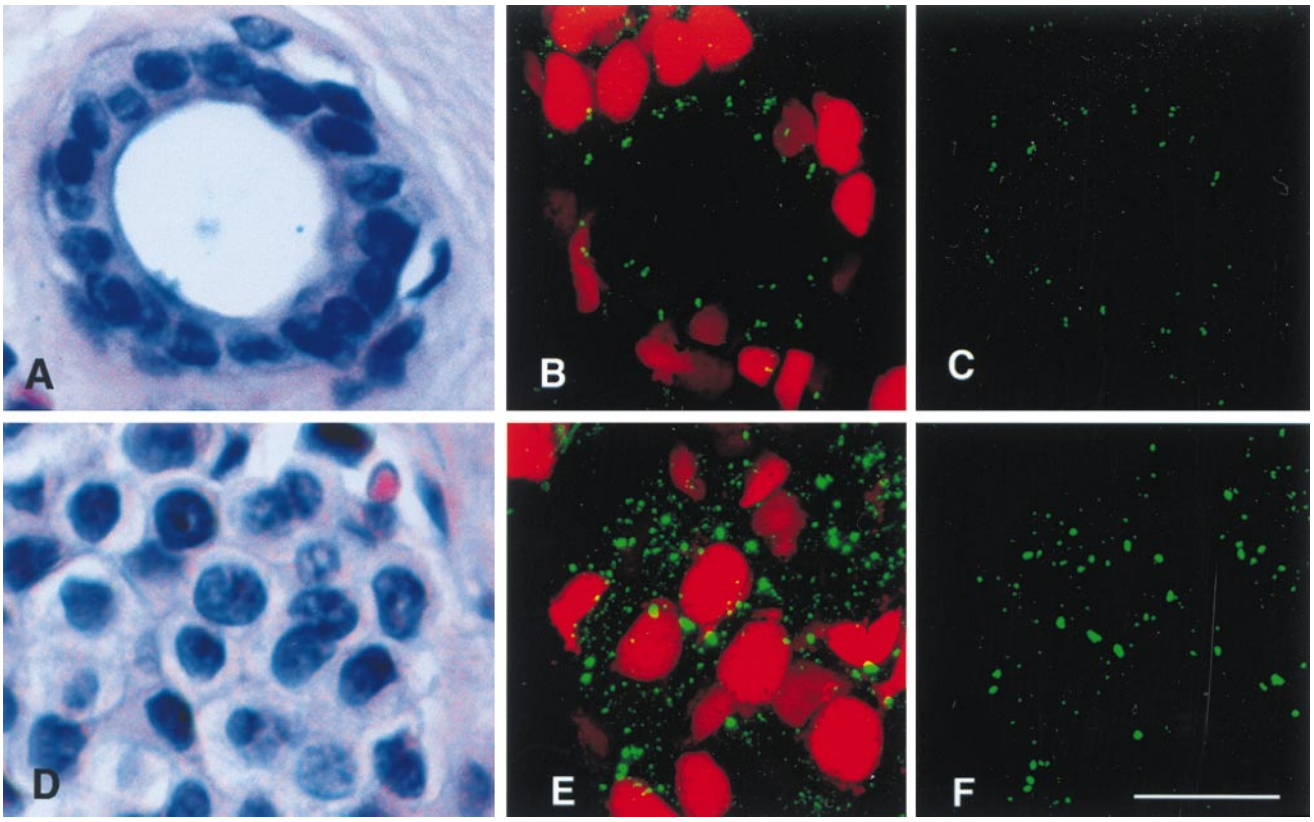

FIG. 1. Centrosome number and size in normal breast duct epithelia (*A–C*) and adenocarcinoma cells (*D–F*). Hematoxylin and eosin-stained paraffin sections of a normal human breast duct (*A*) and a breast adenocarcinoma (*D*). (*B*) Confocal image stack of a normal breast duct stained for centrioles with anticentrin mAb 20H5 (fluorescein isothiocyanate secondary antibody) and for nuclear DNA with propidium iodide. Approximately 20 pairs of centrioles are located apical to the nuclei of epithelial cells that line this normal duct. (*C*) Binary processed image showing the volume of centrin labeling for the same normal epithelial image stack shown in *B*, from which a portion of the data in Table 1 was derived. (*E*) Confocal image stack of a breast adenocarcinoma stained as above. Many large centrin-staining spots mark the location of abnormal centrosomes in the tumor tissue. (*F*) Binary processed image showing the volume of centrin labeling for the same tumor image stack shown in *E*, from which a portion of the data in Table 1 was derived. (Bar = 20 μm.)

tumor cells are significant [Wilcoxon rank sum test (30), $P < 0.005$]. Normal cells contain a mean number of 1.5 centrin-stained spots (corresponding to centrioles) per cell; in contrast, tumor cells contain two-to-four times this number of significantly larger centrin-stained spots per cell (Table 1*A*). Centrin staining of tumor centrosomes is, therefore, more pervasive than expected for staining of individual centrioles and is likely to represent labeling of excess pericentriolar material observed by electron microscopic examination (see below and refs. 10, 18, and 19).

Staining of a second well characterized centrosome marker, γ-tubulin (Fig. 2 *A* and *C*), also demonstrates abnormal centrosome size and number in tumor cells. Furthermore, in double-labeled preparations, centrin and γ-tubulin staining nearly coincide (Fig. 2 *B–D*), suggesting that excessive centrosome size may be the result of general accumulation of centrosomal proteins in tumor cells.

Centrosomes of normal and tumor cells also were examined by transmission electron microscopy (Fig. 3). Normal epithelial cells had two apically positioned centrioles with sparse electron-dense pericentriolar material (Fig. 3 *A–B*). In contrast, tumor cell centrosomes are characterized by multiple centrioles (range = 2–12) surrounded by abundant densely staining pericentriolar material (Fig. 3 *C–E*).

Quantitative analysis of electron micrographs demonstrated that tumor cells have larger numbers of centrioles than do normal cells; the number of centriole profiles seen in an individual ≈900 Å-thick section of normal cells ranged from 0–2 per section, whereas the range seen in individual tumor cell sections of the same thickness is 0–5 per section (Fig. 3*E*; Table 1*B*). Although a single section can reveal the two centrioles present in normal cells, it is unlikely that a single section will reveal all of the centrioles within a given tumor cell. We have observed up to 12 centrioles in individual tumor cells by examining serial sections, whereas in normal controls >2 centrioles were never observed (Table 1*B*; data not shown). Tumor centrosomes, therefore, were characterized by a larger

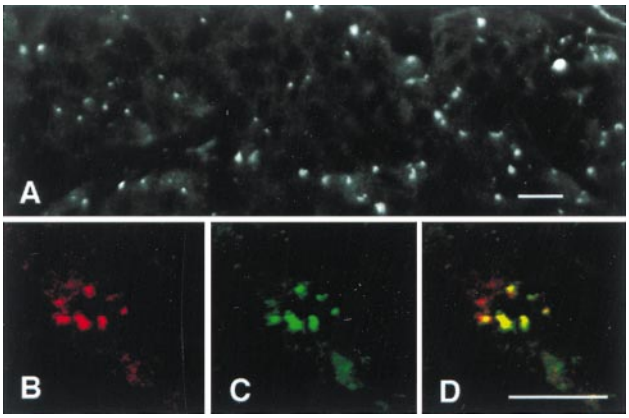

FIG. 2. Immunofluorescence of γ-tubulin in tumor centrosomes. (*A*) In this overview of a breast tumor cryosection, γ-tubulin appears as many large spots scattered randomly throughout the tumor, similar to the distribution of centrin in Fig. 1*E*. Double labeling (*B–D*) of tumor centrosomes by using antibodies to centrin (*B*, red) and γ-tubulin (*C*, green) show virtual coincidence of signal (*D*, yellow). (Bar = 20 μm.)

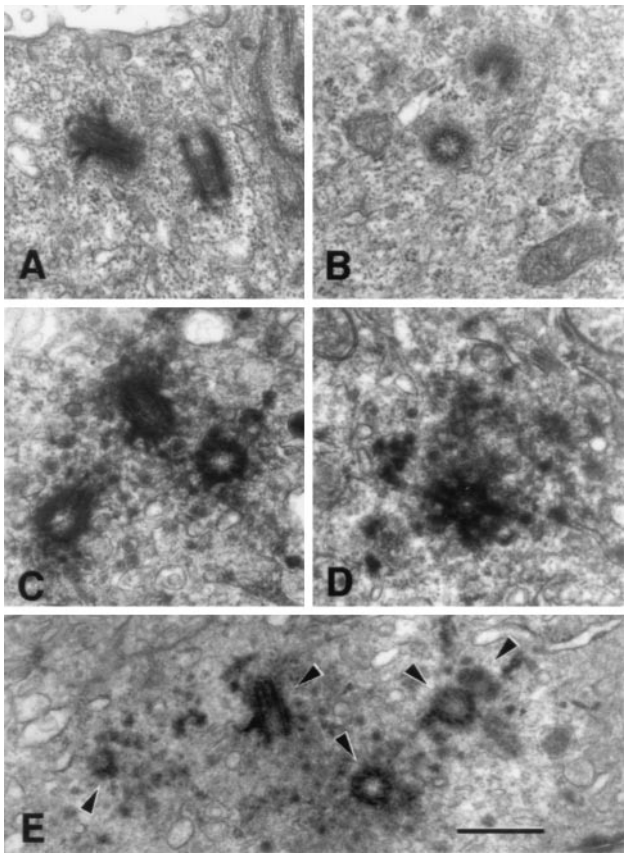

FIG. 3. Normal and tumor centrosome ultrastructure. Electron micrographs of thin sections of normal epithelial cell centrosomes (*A–B*) and centrosomes of tumor cells (*C–E*). (*A*) A normal epithelial cell centrosome illustrating the orientation of the pair of centriole cylinders and sparse pericentriolar material surrounding them. (*B*) A centrosome of another normal breast epithelial cell illustrating two centriole profiles and sparse pericentriolar material. The three tumor cell centrosomes illustrated in *C–E* show large accumulations of densely staining pericentriolar material with numerous centrioles and procentrioles. (*E*) A section of a tumor centrosome that includes five centriole and procentriole profiles (arrowheads). (Bar = 0.5 μm.)

number of centrioles and an excess of electron-dense pericentriolar material.

Centrosomes in tumor cells also displayed anomalous phosphorylation of centrosomal proteins. A polyclonal antibody, αHPC, was raised against the carboxyl-terminal 13 amino acids of human centrin in which the serine representing residue 170 was phosphorylated. Western blot analysis showed that αHPC identifies exclusively phosphorylated, but not nonphosphorylated, centrin (Fig. 4*A*, compare gel lanes *a*, *a′* and *b*, *b′*). αHPC also recognized phosphocentrin in whole cell extracts of human breast tumors (Fig. 4*A*, compare gel lanes *c* and *d*). Indirect immunofluorescence using αHPC demonstrated that normal breast epithelia (Fig. 4*B*) stain sparsely, if at all, whereas for five tumor specimens that we examined, >80% of the tumor cells showed intense centrosome staining (Fig. 4*C*). Indirect immunofluorescence using αHPC revealed bright staining of spindle poles in mitotic cells of the normal immortal breast epithelial cell line MCF10A (25) (Fig. 4*D*), whereas interphase MCF10A centrosomes did not stain (Fig. 4*E*). Taken together, these results indicate that, in normal breast epithelial cells, centrin was normally phosphorylated only during mitosis and not during interphase. In contrast, in breast adenocarcinoma cells, centrin is phosphorylated at inappropriate times during the cell cycle and phosphocentrin accumulates in the unusually large tumor centrosomes.

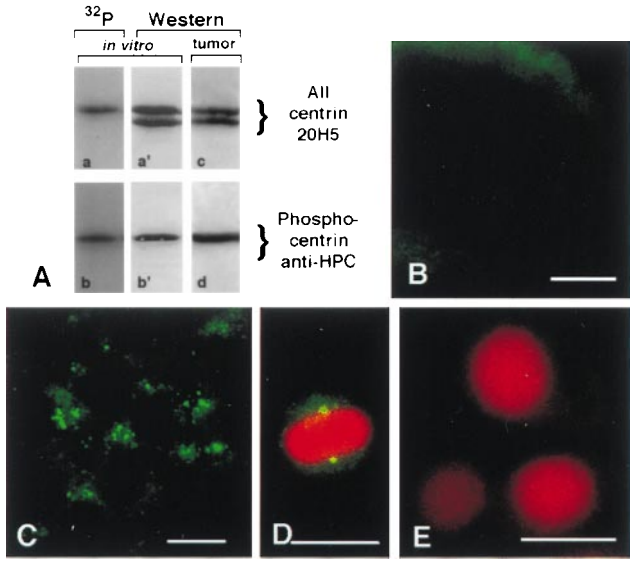

FIG. 4. Inappropriate phosphorylation of breast tumor centrosomes. (*A*) Specificity of αHPC antibodies for phosphocentrin. Western blot analysis of phosphorylated and nonphosphorylated bacterially expressed recombinant centrin (*A*, gel lanes *a′* and *b′*) and autoradiography of the same gel lanes (*A*, gel lanes *a* and *b*). Comparison of the Western blot analysis (*A*, gel lane *a′*) by using mAb 20H5 that reacts with centrin regardless of phosphorylation status and the corresponding autoradiogram (*A*, gel lane *a*) demonstrates that the slower migrating centrin band is phosphorylated. Western blot analysis (*A*, gel lane *b′*) by using αHPC antibody to detect phosphorylated centrin demonstrates reactivity only with the slower migrating form of centrin and no reaction with the nonphosphorylated form. Analysis of whole cell extracts demonstrates that centrin is phosphorylated in breast tumor tissue (*A*, compare gel lanes *c* and *d*). (*B*) A section of a normal breast duct labeled with αHPC antibody demonstrates only a background level of staining in normal epithelial cells. (*C*) A section of a breast adenocarcinoma labeled with αHPC antibody demonstrates that centrosomes stain intensely, indicating that centrin is phosphorylated in tumor cells. (*D–E*) Immunofluorescence of the normal breast epithelial cell line MCF10A stained with αHPC antibody for phosphocentrin and propidium iodide for DNA. The spindle poles of a mitotic cell react strongly with αHPC antibody (*D*), whereas interphase cells show no labeling of their centrosomes (*E*). Tumor centrosome and mitotic MCF10A cell staining with αHPC are completely eliminated with a fivefold excess of competing phosphopeptide (data not shown). (Bar = 20 μm.)

Finally, a simple functional assay was developed to assess the capacity of centrosomes of frozen-sectioned tissues to support microtubule nucleation. Fig. 5*A* illustrates the microtubule nucleating capacity of a normal ductal epithelial cell wherein the apical centrosome nucleated 12–13 microtubules that grew from a single focused MTOC. Fig. 5 *B–C* shows individual cells from touch preparations of normal breast tissues. Normal cells typically nucleate <50 microtubules in this assay (range 0–52; Table 1*C*). In contrast, tumor cells contain multiple MTOCs scattered around the periphery of the nucleus that nucleate significantly larger numbers of microtubules (range 0–270; Fig. 5 *D–F*; Table 1*C*). Fig. 5*D* illustrates a section of a breast tumor where individual centrosomes of most of the cells presented nucleated many microtubules, and Fig. 5 *E–F* show touch preparations of cells from the same tumor. The capacity of interphase tumor cell MTOCs to nucleate an unusually large number of microtubules is characteristic for most tumor cells in a given preparation. As defined by the microtubule nucleation assay described here, tumor cells with multiple MTOCs also have multiple centrin-staining centrosomes.

DISCUSSION

Human breast tumor cells show striking and characteristic abnormalities of several centrosome properties, including ex-

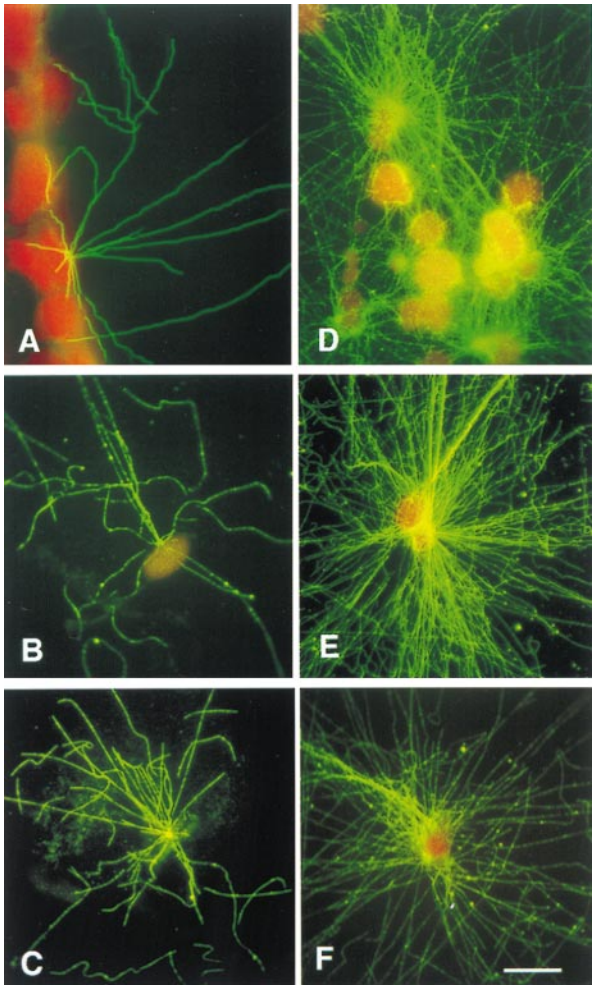

FIG. 5. Tumor centrosomes nucleate more microtubules than do normal epithelial cell centrosomes. (*A*) A section of normal breast tissue after incubation with *Xenopus* egg extract and staining for microtubules. (*D*) A section of a breast tumor illustrating nucleation of large numbers of microtubules by many individual adenocarcinoma cell centrosomes. Touch preparations were analyzed for the purpose of making accurate counts of microtubules nucleated by normal breast epithelial cells (*B–C*) and by tumor cells (*E–F*). Normal breast epithelial cells nucleate <45 microtubules that originate from a single, distinctly focused MTOC (*B–C*). In contrast, tumor cells nucleate many more microtubules that originate from multiple large MTOCs (*E–F*). Microtubules are stained with antitubulin antibodies, and nuclei are stained by using propidium iodide. Data from 50 normal and 50 tumor cells are summarized in Table 1*C*. (Bar = 20 μm.)

cess accumulation of pericentriolar material, supernumerary centrioles, and inappropriate phosphorylation of centrosomal proteins. In addition, tumor centrosomes show functional abnormalities characterized by increased numbers of MTOCs that nucleate unusually large microtubule arrays. Together, these defects in centrosome organization and behavior constitute a condition that we define here as "centrosome hypertrophy". Centrosome hypertrophy is characteristic for 34 of 35 high grade breast adenocarcinoma specimens we have surveyed to date. A careful analysis of nearly 200 additional breast specimens, including ductal carcinoma *in situ*, lobular carcinoma *in situ*, malignant breast tumors of lower histological grade, and fibrocystic disease tissue is currently underway.

In the study presented here, two well characterized centrosomal markers [centrin, and γ-tubulin (31, 32)] demonstrated centrosome hypertrophy in human breast tumor centrosomes. Given the molecular complexity of the centrosome, it is likely that centrosome hypertrophy observed in breast tumor cells involves both accumulation of many centrosomal proteins and their assembly into new centrioles and associated pericentriolar material. Centrosome hypertrophy may result from an increase in centrosome protein expression or a decrease in turnover of centrosome components and/or in recruitment of centrosome precursors from cytoplasmic pools. Centrosome hypertrophy also is likely to be related to perturbation of tumor cell cycle regulatory pathways involved in centrosome duplication (1, 22, 33–35). Anomalous phosphorylation of centrosome proteins in breast tumor cells may be a manifestation of this disregulation of cell cycle controls. Centrosome abnormalities induced by tumor promoters and experimental evidence linking the tumor suppressor p53 to regulation of centrosome dynamics suggest a relationship between centrosome defects and tumor progression (22–24, 33, 36, 37). Although p53 mutation status has yet to be determined for the tumors analyzed in the studies presented here, preliminary experiments suggest that there is not a strict correlation between p53 immunohistochemistry labeling index and centrosome hypertrophy.

Neoplastic transformation is a multistep process that involves activation of protooncogenes, inactivation of tumor suppressor genes, and disregulation of cell cycle checkpoints (38–39). Although the order of these genetic changes may be important for development of certain tumors [for example, colorectal tumors (38)], this importance is not clear for tumors in which progression is less well defined, as is the case for neoplastic transformation of breast epithelia (40). There are at least two functional consequences of centrosome hypertrophy that may play important roles during neoplastic transformation and tumor progression. First, aberrant centrosome duplication may adversely affect maintenance of cell polarity in interphase cells because cytoplasmic architecture and directional vesicular trafficking may be disorganized in a cell with multiple MTOCs. High grade tumors are characterized by the loss of cellular organization, particularly with regard to orientation of adjacent cells relative to one another and to normal cell polarity (together termed "anaplasia") (41). Second, centrosome hypertrophy may increase the incidence of multipolar mitoses, which lead to chromosomal segregation abnormalities and aneuploidy. Aneuploidy is the predominant class of genomic instability found in colorectal, breast, and perhaps solid tumors in general (42–46). Acquisition of such centrosome defects could affect tumor progression by increasing the likelihood of developing further genetic changes that lead to cellular disregulation and metastasis.

These observations have important clinical implications. Given the relationship of centrosome function to cell polarity and to maintenance of genomic integrity, the degree and nature of centrosomal defects may have predictive value with regard to patient prognosis. Tumor cell centrosomes also may present new targets for chemoprevention and development of novel therapeutics.

Finally, the observations presented here are a tribute to Theodor Boveri's prescient depth of understanding of the biology of the centrosome and its relationship to cancer. Ten years after Boveri's death, Maynard Metcalf wrote, "Boveri was the greatest cytologist of his generation . . . a man so keen, so careful and so cautious that any least suggestion from him deserves most thorough consideration. Boveri's work should be the starting point for any studies of causes, inheritance or cure of cancer" (47).

We gratefully acknowledge Ms. Lynn Cordes, Mr. Mark Sanders, the Mayo Electron Microscopy and Optical Morphology Core Facilities, and the Mayo Biomedical Imaging Resource for their technical support, Dr. Vera Suman for assistance with statistical analyses, and Dr. Daniel McCormick for assistance with phosphopeptide synthesis. This research was supported by the Race for the Cure/Twin Cities, the Breast Cancer Research Foundation, the Fraternal Order of Eagles

Cancer Research Fund, the Sitt Foundation, the National Institutes of Health, and the Mayo Foundation.

1. Kellogg, D., Moritz, M. & Alberts, B. (1994) *Annu. Rev. Biochem.* **63,** 639–674.
2. Rieder, C. & Borisy, G. (1982) *Biol. Cell* **44,** 117–132.
3. Wheatley, D. (1982) *The Centriole: A Central Enigma of Cell Biology* (Elsevier Biomedical, Amsterdam).
4. Paintrand, M., Moudjou, M., Delacroix, H. & Bornens, M. (1992) *J. Struct. Biol.* **108,** 107–128.
5. Baron, A. T., Suman, V. J., Nemeth, E. & Salisbury, J. L. (1994) *J. Cell Sci.* **107,** 2993–3003.
6. Wilson, E. B. (1925) *The Cell in Development and Heredity* (Macmillan, New York).
7. Buendia, B., Bré, M.-H., Griffiths, G. & Karsenti, E. (1990) *J. Cell Biol.* **110,** 1123–1135.
8. Rindler, M. J., Ivanov, J. E. & Sabatini, D. D. (1987) *J. Cell Biol.* **104,** 231–241.
9. Errabolu, R., Sanders, M. A. & Salisbury, J. L. (1994) *J. Cell Sci.* **107,** 9–16.
10. Salisbury, J. L. (1995) *Curr. Opin. Cell Biol.* **7,** 39–45.
11. Schiebel, E. & Bornens, M. (1995) *Trends Cell Biol.* **5,** 197–201.
12. Oakley, B., Oakley, C., Yoon, Y. & Jung, M. (1990) *Cell* **61,** 1289–1301.
13. Stearns, T., Evans, L. & Kirschner, M. (1991) *Cell* **65,** 825–836.
14. Zheng, Y., Jung, M. & Oakley, B. (1991) *Cell* **65,** 817–823.
15. Félix, M., Antony, C., Wright, M. & Maro, B. (1994) *J. Cell Biol.* **124,** 19–31.
16. Doxsey, S. J., Stein, P., Evans, L., Calarco, P. D. & Kirschner, M. (1994) *Cell* **76,** 639–650.
17. Brown, C. R., Doxsey, S. J., White, E. & Welch, W. J. (1994) *J. Cell. Physiol.* **160,** 47–60.
18. Baron, A. T., Greenwood, T. M., Bazinet, C. W. & Salisbury, J. L. (1992) *Biol. Cell* **76,** 383–388.
19. Paoletti, A., Moudjou, M., Paintrand, M., Salisbury, J. L. & Bornens, M. (1996) *J. Cell Sci.* **109,** 3089–3102.
20. Boveri, T. (1914) *The Origin of Malignant Tumors*, trans. (1929) (Williams & Wilkins, Baltimore).
21. Murnane, J. P. (1995) *Cancer Metastasis Rev.* **14,** 17–29.
22. Cross, S. M., Sanchez, C. A., Morgan, C. A., Schimke, M. K., Ramel, S., Idzerda, R. L., Raskind, W. H. & Reid, B. J. (1995) *Science* **267,** 1353–1356.
23. Winey, M. (1996) *Curr. Biol.* **6,** 962–964.
24. Fukasawa, K., Choi, T., Kuriyama, R., Rulong, S. & Vande Woude, G. F. (1996) *Science* **271,** 1744–1747.
25. Soule, H. D., Maloney, T. M., Wolman, S. R., Peterson, W. D. Jr., Brenz, R., McGrath, C. M., Russo, J., Pauley, R. J., Jones, R. F. & Brooks, S. C. (1990) *Cancer Res.* **50,** 6075–6086.
26. Murray, A. (1991) *Methods Cell Biol.* **36,** 581–605.
27. Morbeck, D. E., Roche, P. C., Keutmann, H. T. & McCormick, D. J. (1993) *Mol. Cell. Endocrinol.* **97,** 173–181.
28. Perich, J. W. (1992) *Int. J. Pept. Protein Res.* **40,** 134–140.
29. Baron, A. T., Errabolu, R., Dinusson, J. & Salisbury, J. L. (1995) in *Cilia and Flagella,* eds. Dentler, W. & Witman, G. (Academic, San Diego), pp. 341–351.
30. Wilcoxon, F. (1945) *Biometrics* **1,** 80–87.
31. Joshi, H. C., Palacios, M. J., McNamara, L. & Cleveland, D. W. (1992) *Nature (London)* **356,** 80–83.
32. Rao, P., Zhao, J.-Y., Ganju, R. & Ashorn, C. (1989) *J. Cell Sci.* **93,** 63–69.
33. Agarwal, M. L., Agarwal, A., Taylor, W. R. & Stark, G. R. (1995) *Proc. Natl. Acad. Sci. USA* **92,** 8493–8497.
34. Bailly, E., Dorée, M., Nurse, P. & Bornens, M. (1989) *EMBO J.* **8,** 3985–3995.
35. Riabowol, K., Draetta, G., Brizuela, L., Vandre, D. & Beach, D. (1989) *Cell* **57,** 393–401.
36. Mascardo, R. N. & Sherline, P. (1985) *J. Clin. Invest.* **74,** 1186–1192.
37. Wahl, A. F., Donaldson, K. L., Fairchild, C., Lee, F. Y., Foster, S. A., Demers, G. W. & Galloway, D. A. (1996) *Nat. Med.* **2,** 72–79.
38. Vogelstein, B., Fearon, E. R., Hamilton, S. R., Kern, S. E., Presinger, A. C., Leppert, M., Nakamura, Y., White, R., Smits, A. M. & Bos, J. L. (1988) *N. Engl. J. Med.* **319,** 525–532.
39. Hunter, T. & Pines, J. (1994) *Cell* **79,** 573–582.
40. Thor, A. & Yandell, D. (1996) in *Molecular Pathology of Breast Carcinoma*, eds. Harris, J., Lippman, M., Morrow, M. & Hellman, S. (Lippincott-Raven, Philadelphia), pp. 445–454.
41. Lieberman, M. W. & Lebovitz, R. M. (1996) in *Neoplasia*, eds. Damjanov, I. & Linder, J. (Mosby, St. Louis), Vol. 1, pp. 513–547.
42. Lengauer, C., Kinzler, K. & Vogelstein, B. (1997) *Nature (London)* **386,** 623–627.
43. Hartwell, L. (1992) *Cell* **71,** 543–546.
44. Hartwell, L., Weinert, T., Kadyk, L. & Garvik, B. (1994) in *Cell Cycle Checkpoints, Genomic Integrity, and Cancer*, ed. Stillman, B. (Cold Spring Harbor Lab. Press, Plainview, NY), Vol. LIX, pp. 259–263.
45. Visscher, D. W. (1995) *Breast J.* **1,** 222–227.
46. Kallioniemi, O.-P., Hietanen, T., Mattila, J., Lehtinen, M., Lauslahti, K. & Koivula, T. (1987) *Eur. J. Cancer Clin. Oncol.* **23,** 277–282.
47. Metcalf, M. (1925) *J. Am. Med. Soc.* **84,** 1140.